Optimization-Based Calibration of FAST.Farm Parameters Against SOWFA

Preprint

Paula Doubrawa, Jennifer Annoni, and Jason Jonkman
National Renewable Energy Laboratory

Aditya Ghate
Stanford University

Presented at the American Institute of Aeronautics and Astronautics SciTech Forum 2018
Kissimmee, Florida
January 8–12, 2018

NREL is a national laboratory of the U.S. Department of Energy
Office of Energy Efficiency & Renewable Energy
Operated by the Alliance for Sustainable Energy, LLC

This report is available at no cost from the National Renewable Energy Laboratory (NREL) at www.nrel.gov/publications.

National Renewable Energy Laboratory
15013 Denver West Parkway
Golden, CO 80401
303-275-3000 • www.nrel.gov

Conference Paper
NREL/CP-5000-70533
January 2018

Contract No. DE-AC36-08GO28308

NOTICE

This report was prepared as an account of work sponsored by an agency of the United States government. Neither the United States government nor any agency thereof, nor any of their employees, makes any warranty, express or implied, or assumes any legal liability or responsibility for the accuracy, completeness, or usefulness of any information, apparatus, product, or process disclosed, or represents that its use would not infringe privately owned rights. Reference herein to any specific commercial product, process, or service by trade name, trademark, manufacturer, or otherwise does not necessarily constitute or imply its endorsement, recommendation, or favoring by the United States government or any agency thereof. The views and opinions of authors expressed herein do not necessarily state or reflect those of the United States government or any agency thereof.

This report is available at no cost from the National Renewable Energy Laboratory (NREL) at www.nrel.gov/publications.

Available electronically at SciTech Connect http:/www.osti.gov/scitech

Available for a processing fee to U.S. Department of Energy and its contractors, in paper, from:

U.S. Department of Energy
Office of Scientific and Technical Information
P.O. Box 62
Oak Ridge, TN 37831-0062
OSTI http://www.osti.gov
Phone: 865.576.8401
Fax: 865.576.5728
Email: reports@osti.gov

Available for sale to the public, in paper, from:

U.S. Department of Commerce
National Technical Information Service
5301 Shawnee Road
Alexandria, VA 22312
NTIS http://www.ntis.gov
Phone: 800.553.6847 or 703.605.6000
Fax: 703.605.6900
Email: orders@ntis.gov

Cover Photos by Dennis Schroeder: (left to right) NREL 26173, NREL 18302, NREL 19758, NREL 29642, NREL 19795.

NREL prints on paper that contains recycled

Optimization-Based Calibration of FAST.Farm Parameters Against SOWFA

Paula Doubrawa*, Jennifer Annoni†, Jason Jonkman‡
National Renewable Energy Laboratory, Golden, Colorado, 80401, USA
Aditya Ghate§
Stanford University, Stanford, California, 94305, USA

FAST.Farm is a medium-fidelity wind farm modeling tool that can be used to assess power and structural loads contributions of wind turbines in a wind farm. The objective of this paper is to undertake a calibration procedure to set the user-defined parameters of FAST.Farm to accurately represent results from large-eddy simulations. The results provide an in-depth analysis of the comparison of FAST.Farm and large-eddy simulations before and after calibration. The comparison of FAST.Farm and large-eddy simulation results are presented with respect to streamwise and radial velocity components as well as wake-meandering statistics (mean and standard deviation) in the lateral and vertical directions under different atmospheric and turbine operating conditions.

Nomenclature

γ	Yaw Angle, [°]
V_i	Flow Speed Along ith Direction, [m s^{-1}]
δ	Velocity Deficit, [m s^{-1}]
x	Axial (i.e., downstream) Direction, [m]
y	Lateral (i.e., cross-stream) Direction, [m]
z	Vertical Direction, [m]
r	Radial Direction, [m]
θ	Azimuthal Direction, [m]
t	Time, [s]
D	Rotor Diameter, [m]
Δ	Error Norm, [-]
κ	Wave Number, [m^{-1}]

I. Introduction

The majority of research in wind farm aerodynamics to date has been performed with steady[1,2] or quasi-steady[3,4] wind turbine (WT) wake models that are computationally inexpensive and can therefore be run for a variety of atmospheric and WT operating conditions. However, some instances require a higher level of fidelity modeling so that the WT dynamic response to the flow can be accurately evaluated and used in direct applications (i.e., for control analysis and design purposes). For these and other cases in which a wide range of flow scales are relevant, higher-fidelity simulations can be performed using unsteady Reynolds-Averaged Navier-Stokes[5] or large-eddy simulations[6] (LES) of the atmospheric boundary layer coupled to a structural dynamics model for the WT response. The level of computational requirement in the latter approach limits its applicability, and high-resolution, high-fidelity wind farm simulations are often performed for short time

*Research Engineer, National Wind Technology Center, Paula.Doubrawa@nrel.gov
†Research Engineer, National Wind Technology Center
‡Senior Engineer, National Wind Technology Center, AIAA Professional Member
§Graduate Student, Department of Aeronautics and Astronautics, Stanford University

This report is available at no cost from the National Renewable Energy Laboratory at www.nrel.gov/publications.

periods (i.e., 10-20 minutes) and for a small number of idealized scenarios. There is a need for a low-cost medium-fidelity tool that will enable a large number of simulations to be performed over spatial domains that encompass entire wind farms, at relatively high spatial and temporal resolutions [e.g., $\mathcal{O}(10^1)$ m and ~ 1 s] and for longer time periods (e.g., 1 hour) than what is typically achieved with LES.

FAST.Farm[7] is a new multi-physics tool that addresses these needs. Its potential to predict power performance and structural loads within a wind farm makes it a valuable tool for research and industry when seeking to optimize wind farm performance and reliability and reduce uncertainty in annual energy production (AEP) estimates, which remains one of the main challenges in wind engineering.[8] While other medium-fidelity tools have been proposed[9,10] to address this gap between low- and high-fidelity models, FAST.Farm is unique in that it combines the strengths of several well-established modeling tools into a single code. Namely, it complements the controls capabilities of FLORIS,[2,11] incorporates the aero-hydro-servo-elastics functionality of FAST,[12] and includes a wake model implementation that is based on the Dynamic Wake Meandering model,[13] while addressing some of its limitations (e.g., by the inclusion of wake deflection and advection). Moreover, FAST.Farm is used to model the full wind farm, including all WTs, wake and array effects, and a super controller.

With that in mind, the overarching objective of the present work is to calibrate these parameters with reference to high-fidelity LES performed for a single WT in yawed and non-yawed conditions and under a variety of atmospheric conditions. The wake dynamics within FAST.Farm are affected by a set of parameters defined by the user upon initialization. These parameters appear in the three sub-modules of the wake dynamics module as defined in Jonkman et. al.:[7] (i) wake advection, deflection, and meandering; (ii) near wake correction; and (iii) wake deficit increment. In (i), the parameters control the low-pass time filter applied to the rotor boundary conditions at each time step, and the magnitude of the horizontal wake deflection correction. In (ii), a user-specified constant modulates the wake expansion and axial induction in the pressure gradient zone directly behind the WT. In (iii), a set of parameters tailors the eddy viscosity formulation used to close the mass and momentum balance equations, which are solved via the axisymmetric, quasi-steady thin shear layer approximation,[14] and one parameter is used in the wake diameter calculation (plus the choice of wake diameter calculation model). An additional parameter is used for wake meandering (plus the choice of wake-meandering model). Understanding the relationship between these parameters and the modeled wake dynamics is crucial to the development of FAST.Farm so that the model can provide robust solutions under a wide range of atmospheric and turbine operation conditions.

The calibration is based on wake characterization metrics and is performed via a sequential grid search, as described in Section II. The calibrated parameters resulting from this work will be used for the subsequent FAST.Farm validation, which will consider other atmospheric conditions, multiple wakes, and large wind farms. The ultimate objective of the calibration procedure is to provide the FAST.Farm user with default values that can produce simulations of similar accuracy to LES for a wide range of scenarios, and with guidelines for modifying the default values according to the conditions being simulated. Results are presented in Section III and followed by a summary and discussion in Section IV.

II. Methodology

A. Simulations

Simulations of the atmospheric boundary layer are performed with the National Renewable Energy Laboratory's (NREL's) LES-based Simulator fOr Wind Farm Applications (SOWFA)[15] and subsequently used as initial and boundary conditions for SOWFA and FAST.Farm simulations on a domain with one WT. These WT simulations are then used in the calibration of FAST.Farm. Hereinafter, the simulations performed without a WT in the domain are referred to as "freestream simulations" and those performed with a WT as "wake simulations."

1. Freestream Simulations

All freestream simulations are performed with SOWFA and have a mean hub height wind speed $u_{hub} = 8\,\mathrm{m\ s^{-1}}$ along the streamwise (x) direction and $v_{hub} = w_{hub} = 0\,\mathrm{m\ s^{-1}}$ along the cross-stream (y) and vertical (z) directions. Four freestream scenarios are defined: unstable (`U`), neutral (`N`), stable (`S`), and stable with high shear (`SHS`). The turbulence intensity and power law shear exponent of these four scenarios are given in Table 1. The stability and target turbulence intensity in these simulations are modulated by specifying

This report is available at no cost from the National Renewable Energy Laboratory at www.nrel.gov/publications.

a surface heat flux or potential temperature profile up to an assumed atmospheric boundary layer height, depending on the case. Specifying a heating or cooling rate allows the momentum and temperature to develop naturally throughout the boundary layer, but this flux rate is not known a priori, and certain atmospheric conditions in terms of turbulence intensity and stratification cannot be directly obtained through this approach. Alternatively, a generic temperature profile may be directly specified to enforce a required stability condition through height-varying source terms.[16]

Table 1: Simulation scenarios considered in the FAST.Farm and SOWFA simulations with wind turbines (i.e., "wake simulations").

Scenario	Atmospheric Stability	Turbulence Intensity	Shear Exponent	Yaw
`U`	Unstable	10 %	0.1	0°
`N`	Neutral	10 %	0.2	0°
`S`	Stable	5 %	0.2	0°
`SHS`	Stable	10 %	0.4	0°
$\texttt{N}_{\texttt{-25}}$	Neutral	10 %	0.2	-25°
$\texttt{N}_{\texttt{-10}}$	Neutral	10 %	0.2	-10°
$\texttt{N}_{\texttt{+10}}$	Neutral	10 %	0.2	10°
$\texttt{N}_{\texttt{+25}}$	Neutral	10 %	0.2	25°
$\texttt{N}_{\texttt{step}}$	Neutral	10 %	0.2	Stepped (0°–10°–25°)

The freestream simulations are performed on a uniform mesh with a spatial resolution of 10 m. The size of the domain was determined based on the conditions being simulated and is largest for the `U` case in order to allow for the development and evolution of large-scale turbulence structures. These freestream flow fields are then used as inflow for SOWFA wake simulations, and for FAST.Farm wake simulations. For the latter case, the flow is saved at two resolutions as required by FAST.Farm: a low-resolution domain used for meandering wakes (of larger size, on a coarser mesh) and a high-resolution domain used for local inflow to a rotor (of smaller size, on a finer mesh). For the purposes of the calibration study, the spatial resolution is kept fixed at 10 m for the low- and high-resolution domains. The temporal resolution is chosen to be 2 s and $\frac{1}{3}$ s for the low- and high-resolution domains, respectively.

2. Wake Simulations

All wake simulations use the NREL 5-MW WT[?] model. Each of the four freestream simulation scenarios is used as inflow for wake simulations with no yaw error. The `N` scenario is additionally used to drive five wake simulations with fixed ($\texttt{N}_{\texttt{-25}}$, $\texttt{N}_{\texttt{-10}}$, $\texttt{N}_{\texttt{+10}}$, $\texttt{N}_{\texttt{+25}}$) and stepped ($\texttt{N}_{\texttt{step}}$) yaw. The stepped-yaw simulation starts at $\gamma = 0°$ and, after 25% of total simulation time elapsed (450 s), yaws to $\gamma = 10°$ where it remains for another 17% of the total simulation time (300 s) before yawing to $\gamma = 25°$ (these times are reported after the start-up transient period). These simulations make for a total of nine wake scenarios (Table 1) that are modeled once using SOWFA and many times using FAST.Farm during the calibration procedure. One FAST.Farm simulation takes on the order of 1 hour to run in serial mode on a desktop computer with a single core while one SOWFA simulation takes on the order of 2 days to run with 600 cores. Fig. 1 shows the flow field computed from FAST.Farm (top) and SOWFA (bottom). For the present work, all wake simulation outputs are analyzed for a period of 1,800 s (after a 200-s start-up transient period), at a 2-s sampling resolution, and in a meandering frame of reference (i.e., a coordinate system following the wake center). The SOWFA simulated flow is saved at the same temporal frequency, but the spatial resolution of the flow fields in the wake is higher than in FAST.Farm, as evidenced by Fig. 1. More specifically, the SOWFA simulations are performed on a 10-m mesh with two inner refinement zones of 5 m and 2.5 m.

The wake simulations performed with SOWFA and FAST.Farm are equivalent in that they make use of the same WT model, and the same ambient wind data set for initial and boundary conditions. These precursor freestream simulations have a much lower computational cost than performing LES of a domain with WTs, which warrants the use of a WT model, and the coupling between the fluid dynamics and the aero-servo-elastics solvers. The advantage of uncoupling the fluid and structural dynamics solvers is that for a fixed atmospheric scenario, the same inflow data can be used to perform countless FAST.Farm simulations

This report is available at no cost from the National Renewable Energy Laboratory at www.nrel.gov/publications.

in which the WT model (i.e., design and control) and wind-farm configuration can be modified. While this is in theory possible with LES codes, their associated computational cost precludes the use of such an approach with high-fidelity models. Currently, these precursor freestream LES are a necessary step to running FAST.Farm, but development is underway to also accommodate the use of synthetic wind data (e.g., from TurbSim[17]).

In addition to the numerics, other major differences between SOWFA and FAST.Farm pertain to the underlying models for the flow field and for the WT. SOWFA solves the spatially filtered incompressible Navier-Stokes equations with a Boussinesq buoyancy term. The buoyancy requires that the spatially filtered potential temperature transport be also solved. The equations are closed with the Deardorff/Lilly one-equation subfilter-scale turbulence model,[6] while FAST.Farm implements the quasi-steady axisymmetric formulation of the thin shear layer approximation to Navier-Stokes and closes the system with an eddy-viscosity model.[14] In terms of the WT, SOWFA uses an actuator line model[18] with rotating blades while FAST.Farm is based on Blade Element Momentum theory.[7] A consequence of these differences is that wake meandering in SOWFA is a direct result of the ambient and wake-induced turbulence present in the solution, while in FAST.Farm the wake is meandered laterally and axially based on the spatially averaged velocity of the freestream flow local to the wake. Finally, merging of wakes (though not considered in this paper) is also a direct consequence of flow advection and diffusion within SOWFA, but treated differently within FAST.Farm where axial deficits are superimposed with the root-sum-squared method and radial deficits by a vector sum in zones of wake overlap.

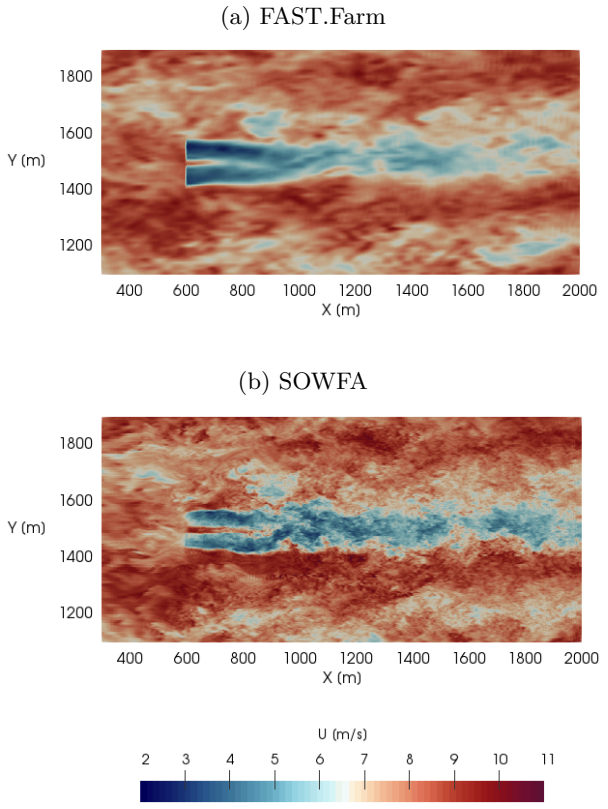

Figure 1: Example instantaneous flow fields of the streamwise velocity component at hub height produced by FAST.Farm (a) and SOWFA (b) under neutral stratification inflow. The SOWFA flow field exhibits finer detail due to the use of a finer spatial resolution in its solution.

B. Calibration Parameters

We seek to calibrate 18 parameters, which are found in the "wake dynamics" and "ambient wind and array effects" modules of FAST.Farm. The first guess values for each parameter and the wake simulations used for their calibration are given in Table 2. The initial guesses are based on values found in literature, and on previous wake-modeling efforts. For each parameter being calibrated, only a subset of the wake-simulation scenarios is relevant. To determine which scenarios will be used for each parameter being calibrated, the parameters were combined into groups: "Offset," "Eddy Viscosity and Near Wake," "Ambient," "Shear," "Meandering," and "Transient." The grouping is done to reduce the number of simulations that need to be conducted during the grid searches (see Section D) and is based on the physics that are most relevant for the parameters being calibrated. Note that the `N` simulation scenario is included in all groups, to ensure that the calibration does not improve FAST.Farm results under a specific physical setting at the cost of its performance under the reference condition of neutral atmosphere and zero yaw offset. These groups are calibrated sequentially, as will be further discussed in Subsection D.

The parameters related to the correction for horizontal wake deflection were assigned to the "Offset" group. They define the wake offset at the rotor (C^{O}_{HWkDfl}), at the rotor scaled with yaw error (C^{OY}_{HWkDfl}), scaled with the downstream distance (C^{x}_{HWkDfl}), and scaled with both yaw error and downstream distance (C^{xY}_{HWkDfl}).

This report is available at no cost from the National Renewable Energy Laboratory at www.nrel.gov/publications.

$C_{NearWake}$ adjusts the wake deficit correction for the pressure gradient zone directly behind the rotor in the near wake, and was placed in the "Eddy Viscosity and Near Wake" group along with k_{vAmb} and k_{vShr}, which modulate the relative contribution of the ambient and wake shear layer turbulence to the eddy viscosity.

The eddy viscosity equation accounts for the influence of ambient turbulence and of the wake shear layer on the flow. Each of these components includes a filter function, which is modulated by a set of four parameters defining the function minimum ($C_{vAmb,FMin}$ and $C_{vShr,FMin}$), regulating the downstream location where the function transitions from this minimum value to an exponential region ($C_{vAmb,DMin}$ and $C_{vShr,DMin}$), determining the rate of change in the exponential region ($C_{vAmb,Exp}$ and $C_{vShr,Exp}$), and finally regulating the downstream location where the functions transition to their maximum value of 1 ($C_{vAmb,DMax}$ and $C_{vShr,DMax}$), which effectively eliminates the filter. Because each set of four parameters defines a function, they are combined into their own groups: "Ambient" (for C_{vAmb}) and "Shear" (for C_{vShr}).

The "Meandering" group includes $Mod_{Meander}$ and $C_{Meander}$, which define the weighted spatial averaging method (i.e., a spatial filter model) for wake meandering and the cut-off wave number for the filter. Finally, f_c is calibrated on its own in the category "Transient" and defines the cutoff frequency for the low-pass time filter used in the wake advection, deflection, and meandering module and to ensure high-frequency fluctuations do not pass into the quasi-steady wake-deficit increment model. Note that wake diameter calculation parameters ($Mod_{WakeDiam}$ and $C_{WakeDiam}$) are not included in the calibration procedure. Instead, $Mod_{WakeDiam} = 1$ is used throughout (i.e., the wake diameter is set to the rotor diameter).

Table 2: FAST.Farm parameters being calibrated, first-guess values, SOWFA wake simulations used in the calibration of each parameter, and parameter groups defined for the calibration procedure in the order that they are calibrated.

FAST.Farm Parameter	First Guess	Unit	Wake Simulations Used	Parameter Group
C^{O}_{HWkDfl}	-2.9	[m]	N, N_{-25}, N_{-10}, N_{+10}, N_{+25}	Offset
C^{OY}_{HWkDfl}	-0.24	[m/°]	N, N_{-25}, N_{-10}, N_{+10}, N_{+25}	Offset
C^{x}_{HWkDfl}	-0.0054	[-]	N, N_{-25}, N_{-10}, N_{+10}, N_{+25}	Offset
C^{xY}_{HWkDfl}	0.00039	[1/°]	N, N_{-25}, N_{-10}, N_{+10}, N_{+25}	Offset
k_{vAmb}	0.07	[-]	S, N, U, SHS	Eddy Viscosity and Near Wake
k_{vShr}	0.018	[-]	S, N, U, SHS	Eddy Viscosity and Near Wake
$C_{NearWake}$	2.0	[-]	S, N, U, SHS	Eddy Viscosity and Near Wake
$C_{vAmb,DMin}$	0.0	[-]	S, N, U, SHS	Ambient
$C_{vAmb,DMax}$	2.0	[-]	S, N, U, SHS	Ambient
$C_{vAmb,FMin}$	0.0	[-]	S, N, U, SHS	Ambient
$C_{vAmb,Exp}$	1.0	[-]	S, N, U, SHS	Ambient
$C_{vShr,DMin}$	2.0	[-]	S, N, U, SHS	Shear
$C_{vShr,DMax}$	11.0	[-]	S, N, U, SHS	Shear
$C_{vShr,FMin}$	0.035	[-]	S, N, U, SHS	Shear
$C_{vShr,Exp}$	0.4	[-]	S, N, U, SHS	Shear
$Mod_{Meander}$	1	[-]	S, N, U, SHS	Meandering
$C_{Meander}$	2.0	[-]	S, N, U, SHS	Meandering
f_c	0.003	[Hz]	N, N_{step}	Transient

C. Simulations Cross-Comparison Metrics

The calibration procedure is based on calculated differences between the FAST.Farm simulations and the reference high-fidelity wake simulations performed with SOWFA. These differences are computed at nine discrete distances downstream of the WT between 2 and 10 rotor diameters (D) at 1-D intervals. For a given variable X, these differences are computed as $X_{FF} - X_S$ where the FF and S subscripts denote FAST.Farm and SOWFA values, respectively.

This report is available at no cost from the National Renewable Energy Laboratory at www.nrel.gov/publications.

The variables considered are: temporal mean of radial distribution of axial velocity deficit $\overline{\delta V}_x(r,x)$, temporal mean of radial distribution of radial velocity deficit $\overline{\delta V}_r(r,x)$, temporal mean of magnitude of wake center radial displacement relative to the WT hub $\mu_{wake}(x)$, and standard deviation of magnitude of wake center radial displacement relative to the WT hub $\sigma_{wake}(x)$. All of these variables are directly output by FAST.Farm, but must be computed separately for SOWFA. Note that the data extraction planes are slightly different between the two models likely resulting in subtle differences between the diagnosed wake metrics (e.g., the planes in FAST.Farm are parallel with the 5-degree tilt of the rotor whereas this tilt is not included in SOWFA; and during the transient case, the planes in SOWFA are analyzed at discrete yaw orientations of 0°, 10°, and 25° whereas the orientations of the planes in FAST.Farm vary in time according to the transient yaw motion).

The radially dependent mean velocity deficits in the axial and radial directions are output by FAST.Farm for a number of radial nodes specified by the user. For the FAST.Farm simulations in this study, computations are performed on 40 nodes between $r = 0$ m and $r = 195$ m, with equal spacing $\Delta r = 5$ m. Half of these nodes are selected to be included in the model output, with more points concentrated near the hub where the largest gradients in wake deficit are found. To enable a comparison between the axisymmetric FAST.Farm deficit and the asymmetric SOWFA values, the SOWFA output is post-processed for each distance downstream considered, carrying out the following steps:

(i) Estimate vertical profile of freestream wind speed and use it to obtain velocity deficits $\delta u(x,y,z,t)$, $\delta v(x,y,z,t)$, and $\delta w(x,y,z,t)$;

(ii) Identify wake edge and wake center $y_{wake}(x,t)$ and $z_{wake}(x,t)$;

(iii) Use wake center to go from fixed frame of reference to meandering frame of reference;

(iv) Sample radial and axial flow deficits at various radial distances from wake center to edge of sampled plane, at 12 different azimuthal directions to obtain $\delta V_x(r,\theta,x,t)$ and $\delta V_r(r,\theta,x,t)$;

(v) Azimuthally average the sampled deficits to obtain $\delta V_x(r,x,t)$ and $\delta V_r(r,x,t)$;

(vi) Interpolate to the same radial nodes defined in FAST.Farm;

(vii) Temporally average deficits to obtain $\overline{\delta V}_x(r,x)$ and $\overline{\delta V}_r(r,x)$.

The mean and standard deviation of the wake center radial displacement from the WT hub are also considered in the calibration. These values are directly output by FAST.Farm but are once again diagnosed from SOWFA output by tracking the temporal evolution of the wake center position at each downstream distance. This is done with steps (i) and (ii) outlined above and using NREL's Simulated And Measured Wake Identification and CHaracterization (SAMWICh) toolbox. Note that only the total radial magnitude of the wake movement is considered at each realization, and horizontal and vertical meandering are not treated separately in the parameter optimization procedure.

Because the calibration is based on wake characteristics, it is important to ensure that the WT thrust is reasonably matched between both models. Thrust values are shown in Fig. 2 for FAST.Farm and SOWFA for the scenarios without yaw error (`S`, `N`, `U`, and `SHS`). The temporal mean of the thrust differences between SOWFA and FAST.Farm stayed below $\sim 1\%$ for all cases with $\gamma = 0°$ (those shown in Fig. 2) and with $|\gamma| = 10°$ ($\texttt{N_10}$, $\texttt{N+10}$) and below $\sim 7\%$ for the cases with $|\gamma| = 25°$ ($\texttt{N_25}$, $\texttt{N+25}$, $\texttt{N}_{\texttt{step}}$). The variation of thrust about the mean compares quite reasonably between FAST.Farm and SOWFA, with a slight overprediction in thrust standard deviation by FAST.Farm. This overprediction is believed to be the result of the absence of a dynamic wake model within FAST, which would lead to a delay in how the induction reacts to changes in the inflow or loads. In general, the dynamic wake has a filtering effect on turbine loads and is intrinsically included in the SOWFA solution.

D. Optimization

In the calibration procedure, we seek to minimize the norm of the differences between the wake characterization metrics produced by FAST.Farm and those diagnosed from SOWFA output, as described in Subsection C. In other words, we seek to minimize the total error norm,

This report is available at no cost from the National Renewable Energy Laboratory at www.nrel.gov/publications.

$$\Delta_{total} = \sum_{sim=1}^{sim=\mathrm{N_{sim}}} \Delta_{sim} \tag{1a}$$

$$\Delta_{sim} = \left[\Delta\overline{\delta V}_x + \Delta\overline{\delta V}_r + \Delta\mu_{wake} + \Delta\sigma_{wake}\right] \tag{1b}$$

where Δ_{total} is the sum of the error norms over all simulations included in a given calibration step (1 to N_{sim} where N_{sim} is 2, 4, or 5 depending on the group being calibrated, as indicated in Table 2). The error norms for individual simulations Δ_{sim} are a sum of the error norms of individual wake metrics ($\overline{\delta V}_x$, $\overline{\delta V}_r$, μ_{wake}, and σ_{wake}) as given by

$$\Delta\overline{\delta V}_x = \sum_{2\ \mathrm{D}}^{10\ \mathrm{D}} \left[\frac{\|\overline{\delta V}_{x,FF}(r,x) - \overline{\delta V}_{x,S}(r,x)\|_F}{\|\overline{\delta V}_{x,S}(r,x)\|_F}\right] \tag{2a}$$

$$\Delta\overline{\delta V}_r = \sum_{2\ \mathrm{D}}^{10\ \mathrm{D}} \left[\frac{\|\overline{\delta V}_{r,FF}(r,x) - \overline{\delta V}_{r,S}(r,x)\|_F}{\|\overline{\delta V}_{r,S}(r,x)\|_F}\right] \tag{2b}$$

$$\Delta\mu_{wake} = \sum_{2\ \mathrm{D}}^{10\ \mathrm{D}} \left[\frac{\|\mu_{wake,FF}(x) - \mu_{wake,S}(x)\|_F}{\|\mu_{wake,S}(x)\|_F}\right] \tag{2c}$$

$$\Delta\sigma_{wake} = \sum_{2\ \mathrm{D}}^{10\ \mathrm{D}} \left[\frac{\|\sigma_{wake,FF}(x) - \sigma_{wake,S}(x)\|_F}{\|\sigma_{wake,S}(x)\|_F}\right] \tag{2d}$$

where the summation is done over all downstream distances considered (2 D to 10 D), ($\overline{\ }$) denotes temporal averaging, the FF and S subscripts denote FAST.Farm and SOWFA values, respectively, and $\|\ \ \|_F$ denotes the Frobenius norm.

Each parameter group is calibrated separately, but groups are calibrated sequentially in the order that they appear in Table 2. When a group is being calibrated, several FAST.Farm simulations are performed by varying the value assigned to one parameter within the group at a time. To limit the computational cost of the calibration, a grid-search optimization approach is taken. Namely, values to be tested on each parameter are pre-selected, and all possible combinations of these values are considered. For example, if four test values are selected for each of the four parameters in the "Offset" group, then 256 parameter combinations are possible. Because five wake-simulation scenarios are considered within this group (`N`, `N-25`, `N-10`, `N+10`, `N+25`), this setup requires 1,280 FAST.Farm simulations to be performed. After all of these simulations are complete, Eqs. (2a) to (2d) are used to compute the sum of norms for each one, leading to 1,280 norm values in this example. These Δ_{sim} values are then summed across the five simulations, leading to a total of 256 Δ_{total} values. The combination of parameters that presents the lowest Δ_{total} is then selected as the optimal setup for the group being considered. These optimized parameter values are then fixed, and the next group is calibrated in a similar fashion. This entire procedure is referred to as "sequential grid search."

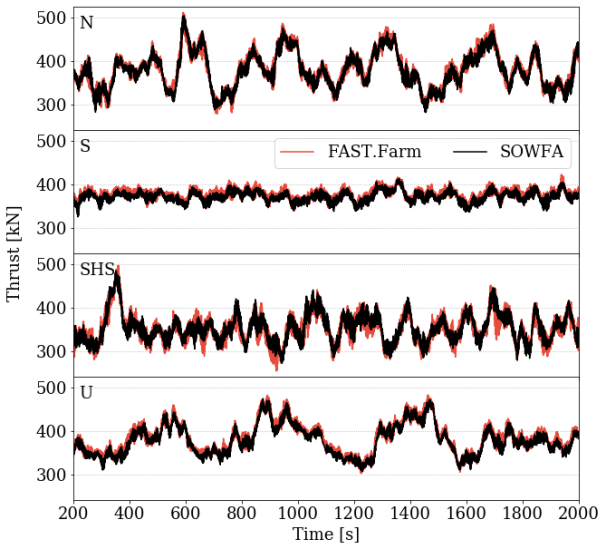

Figure 2: Time series of thrust for FAST.Farm (red) and SOWFA (black) for simulation scenarios `N`, `S`, `SHS`, and `U`.

For the group "Transient", the temporal evolution of wake dynamics is important and differences of temporally-averaged wake quantities [as defined in Eq. (2)] may not be adequate indicators of FAST.Farm performance under a variety of f_c values. Therefore, a different definition of Δ_{sim} is also tested for this group. Within this modified definition, rolling means (computed over 300-s periods) of four quantities are

This report is available at no cost from the National Renewable Energy Laboratory at www.nrel.gov/publications.

considered: radially-averaged V_x and V_r, and lateral and vertical displacement of the wake center relative to the hub. For a given simulation, Δ_{sim} is then computed as the sum of the normalized error norms between FAST.Farm and SOWFA for these four quantities. This modified method captures the transient effect that f_c has on the time series, but yielded the same results as the method used for the other parameter groups (not shown), thus confirming the robustness of the calibration methodology.

Two rounds of the sequential grid search are performed in the present study. Before the first round, all parameters are set to the first-guess values given in Table 2. After the first round, the ranges of values being tested for each parameter are re-evaluated and adjusted based on the intermediate results. A second round is then carried out to obtain the final calibrated values.

III. Results

In this section we analyze the FAST.Farm performance relative to SOWFA for the nine wake scenarios considered before (Section A) and after (Section C) the parameters are calibrated. The optimization results from the sequential grid search are given in Section B. Similarly to the metrics considered in the calibration procedure, the comparison of FAST.Farm and SOWFA is given in terms of wake center statistics and wake deficits.

A. FAST.Farm Simulations with First-Guess Parameter Values

1. Wake Meandering

Wake-meandering statistics in terms of probability density functions (PDFs) of the wake centers from SOWFA and FAST.Farm using the first-guess parameter values are given in Fig. 3. The best performance for both lateral and vertical meandering is seen for the `U` scenario, where both the mean magnitude of meandering and the standard deviation of the distribution are well reproduced by FAST.Farm. Reasonable agreement is also seen for cases `N`, `SHS`, and $\texttt{N}_{\texttt{-10}}$. For case `S`, FAST.Farm produces reasonable estimates of the mean wake center displacement, but underestimates its fluctuations. Note that in the near wake, the meandering fluctuations are low for both FAST.Farm and SOWFA with PDF values that in some cases exceed the limit on the secondary horizontal axis used.

For the fixed-yaw simulations, FAST.Farm tends to overestimate the magnitude of mean wake meandering in the lateral direction. The discrepancies between SOWFA and FAST.Farm increase with downstream distance as the magnitude of the mean wake center displacement keeps increasing for FAST.Farm but quickly saturates near the near-wake value for SOWFA. In the vertical direction the opposite is seen, with FAST.Farm underestimating the mean magnitude of meandering while reproducing well the rate of change of the mean magnitude of meandering with downstream distance. Results for $\texttt{N}_{\texttt{step}}$ indicate a slight underestimation of the mean magnitude of meandering, but similar standard deviation to what is seen in SOWFA. FAST.Farm captures the bi-modal distribution of lateral wake meandering at 2 D, accurately predicting the first peak around a value of 0.0 for the wake motion but over-estimating the mean meandering magnitude for the second peak, which is associated with positive yaw and negative wake deflection. The calibration of the offset parameters and of f_c is expected to improve agreement between both models in terms of the mean wake center movement. Likewise, the calibration of meandering parameters will likely improve the agreement for the wake center fluctuations.

2. Wake Deficit

Radial profiles of wake deficit for FAST.Farm using the first-guess parameter values are given in Fig. 4. For the axial velocity deficits, the error is low for scenarios `N`, `S`, `SHS`, `U`, $\texttt{N}_{\texttt{-10}}$, and $\texttt{N}_{\texttt{+10}}$ across all downstream distances and reflecting the relatively good agreement between FAST.Farm and SOWFA. For the large yaw cases ($\texttt{N}_{\texttt{-25}}$ $\texttt{N}_{\texttt{+25}}$ and $\texttt{N}_{\texttt{step}}$) the errors are largest between 4 and 8 D.

For the radial velocity deficits, all nine simulations present a similar behavior with large error norms in the near wake (2 D to 3 D) due to an overestimation of $\overline{\delta V_r}$ by FAST.Farm. Starting at 4 D, the deficits recover and the agreement between FAST.Farm and SOWFA is good and consistent across all wake-simulation scenarios.

This report is available at no cost from the National Renewable Energy Laboratory at www.nrel.gov/publications.

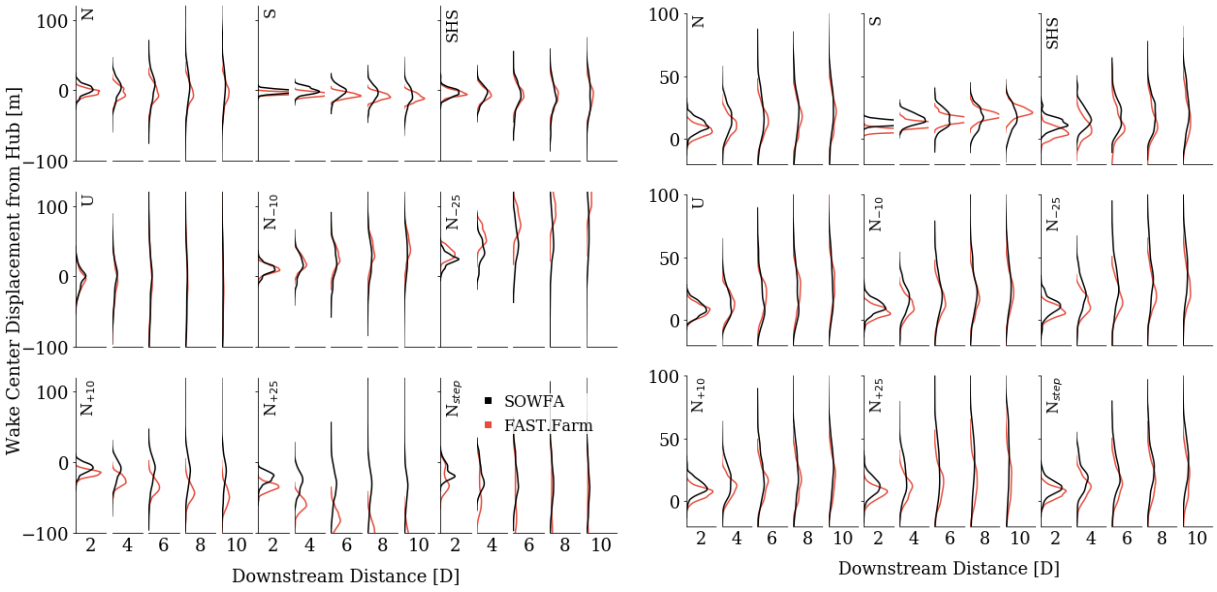

(a) Lateral Meandering

(b) Vertical Meandering

Figure 3: Axial evolution (primary horizontal axis, [D]) of fitted histograms (secondary horizontal axis) of wake center displacement (vertical axis,[m]) relative to WT hub in the lateral (a) and vertical (b) directions for the nine wake-simulation scenarios defined in Table 1 for SOWFA (black) and FAST.Farm (red). Values are for FAST.Farm simulations run with the first-guess parameters. To enable direct comparisons, secondary horizontal axis spans 0.0 to 0.1 m^{-1} in (a) and (b). Vertical axes are uniform within (a) and within (b).

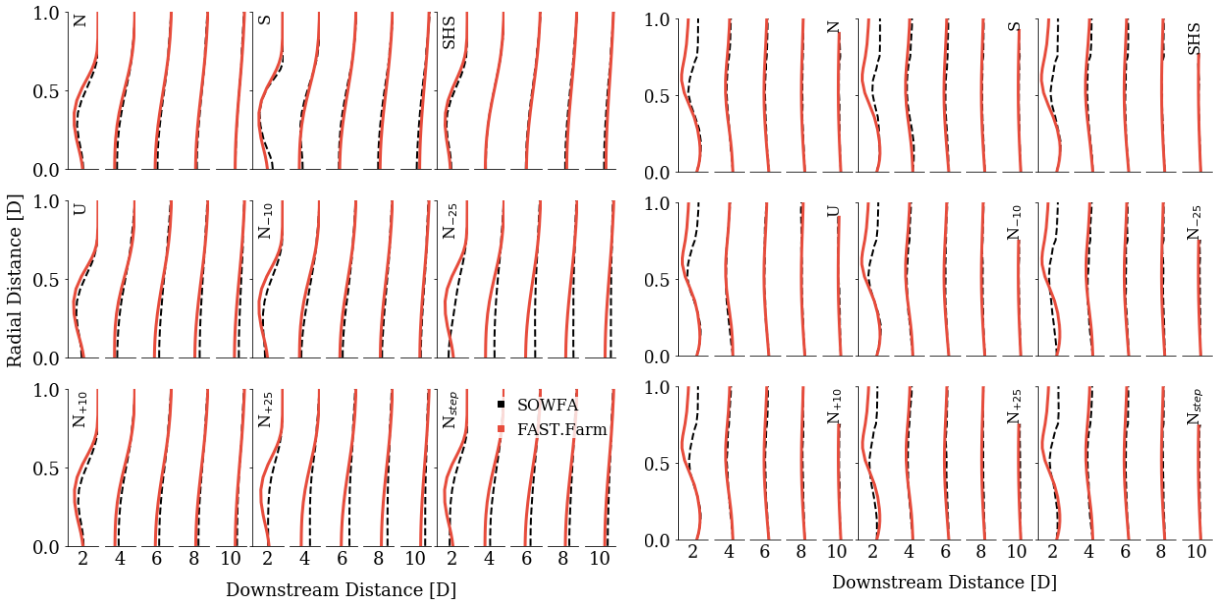

(a) Axial Velocity Deficit

(b) Radial Velocity Deficit

Figure 4: Axial evolution (primary horizontal axis, [D]) of radial distribution (vertical axis, [D]) of temporally averaged velocity deficit (secondary horizontal axis) in the axial (a) and radial (b) directions for the nine wake-simulation scenarios defined in Table 1 for SOWFA (black) and FAST.Farm (red). Values are for FAST.Farm simulations run with the first-guess parameters. Secondary horizontal axis spans -5.5 to 0.1 m s^{-1} in (a) and -0.25 to 0.15 m s^{-1} in (b).

This report is available at no cost from the National Renewable Energy Laboratory at www.nrel.gov/publications.

B. Optimization of FAST.Farm Parameters

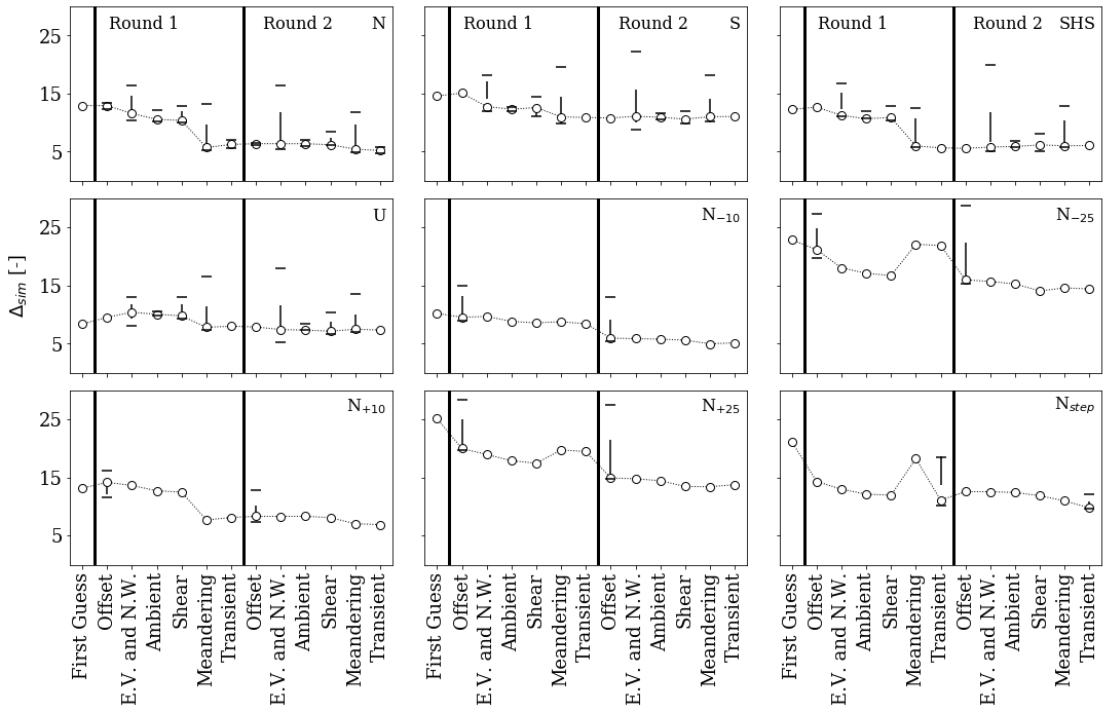

Figure 5: Evolution of error norm for each wake-simulation scenario from first guess to final optimized parameters through the two sequential grid search rounds. Circles indicate the Δ_{sim} [Eq. (1)] of the FAST.Farm simulation with the parameter combination that yields the lowest error norm at the end of each calibration step. Bars give the mean $\pm$ standard deviation of Δ_{sim} across all parameter combinations within a group.

Figure 5 shows the evolution of the total error norm starting with the FAST.Farm simulation performed with the first guess for the parameters, and ending with the FAST.Farm results obtained after all parameters have been calibrated. The circles in Fig. 5 are Δ_{sim} and obtained running FAST.Farm one time and setting the parameters to their optimized values sequentially, as they are updated throughout the calibration procedure. For example, error norms for "Offset" in Round 1 refer to FAST.Farm simulations performed with updated values for the four offset parameters but with first-guess values for all other parameter groups, which are calibrated after the "Offset" group. For each group, the mean and standard deviation of the error norm Δ_{sim} for all parameter combinations is given for each simulation scenario that is considered in the calibration of that group. For the "Offset" group, that includes simulations `N-10`, `N+10`, `N-25`, `N+25`, and `N`. The parameter values tested within each calibration group were centered around the first guess, and are given in Table 3.

For all simulation scenarios, there is a clear trend of decreasing error norm as the calibration procedure advances from "Offset" to "Transient" in Round 1. The final values of Δ_{total} are lower than the starting values for all nine simulation cases (although this result is not obvious when comparing Δ_{sim} values given in Fig. 5). However, because of the large number of atmospheric conditions and yaw set points considered, it is difficult to minimize the error norm of all simulation scenarios at once. The grid search method employed gives equal weight to all parameters and simulation scenarios within a group. As a result, the Δ_{sim} value of a particular simulation may increase within a given calibration step to leverage the improvement obtained for other simulation scenarios considered in that same step. That is particularly evident for the "Meandering" group in Round 1, where error norms increase for cases `N-25`, `N+25`, and `Nstep`but decrease for all simulation scenarios considered most important for this group (the $\gamma = 0°$ cases).

The results obtained with Round 1 of the sequenced grid search indicate error norms that are substantially larger for simulation scenarios with large yaw (`N-25` and `N+25`) than for the other cases, which can potentially be addressed with a more careful calibration of the "Offset" group. We hypothesize that the values and ranges selected for the four offset parameters in Round 1 provide non-unique optimized solutions, depending on the

This report is available at no cost from the National Renewable Energy Laboratory at www.nrel.gov/publications.

simulation scenario being considered and on the values taken by other parameters. Because the SOWFA and FAST.Farm simulations performed for this study do not include the Coriolis effect, we choose to force C^O and C^x to zero in Round 2 of the sequenced search. This can be justified because Coriolis adds a consistent offset to the horizontal wake center position even in conditions of zero yaw. For the present case, this effect does not need to be modeled, and setting these values to zero will allow the calibration methodology to provide robust, unique solutions to the C^{xY} and C^{OY} parameters. After setting $C^O = C^x = 0$, the error norms for Round 2 level off with the "Offset" group and remain fairly constant throughout the calibration of the subsequent groups. This result indicates that the total norm converges at the beginning of Round 2, and that the calibrated parameters chosen with this procedure are robust.

Table 3: Values considered for each parameter in both rounds of the sequenced grid search: range [min,max], number of values within the range n, and optimal value chosen for each parameter at the end of each round. For units, see Table 2. When not given, range and n in Round 2 are the same as in Round 1.

Parameter	Sequenced Grid Search Round 1			Round 2			First Guess
	[min, max]	n	optimal	[min, max]	n	optimal	
C^O_{HWkDfl}	[-4.0, 0.0]	4	0.0	0.0	1	0.0	-2.9
C^{OY}_{HWkDfl}	[-1.0, 0.0]	4	-0.1	[0.0, 1.0]	11	0.3	-0.24
C^x_{HWkDfl}	[-0.005, 0.01]	6	0.005	0.0	1	0.0	-0.0054
C^{xY}_{HWkDfl}	[-0.003, 0.001]	5	-0.001	[-0.01, 0.0]	11	-0.004	0.00039
k_{vAmb}	[0.05, 0.09]	5	0.05	[0.01, 0.09]	9	0.05	0.07
k_{vShr}	[0.010, 0.020]	6	0.014			0.016	0.018
$C_{NearWake}$	[1.2, 2.2]	6	1.8			1.8	2.0
$C_{vAmb,DMin}$	[0.0, 0.5]	4	0.17			0.0	0.0
$C_{vAmb,DMax}$	[1.0, 3.0]	4	3.0	[1.0,5.0]	6	1.0	2.0
$C_{vAmb,FMin}$	[0.0, 1.0]	4	0.0			1.0	0.0
$C_{vAmb,Exp}$	[0.01, 1.0]	4	0.01			0.01	1.0
$C_{vShr,DMin}$	[0.0, 4.5]	4	3.0			3.0	2.0
$C_{vShr,DMax}$	[9.0, 15.0]	4	15.0	[13.0,33.0]	11	25.0	11.0
$C_{vShr,FMin}$	[0.00, 0.10]	4	0.08	[0.0,0.25]	6	0.2	0.035
$C_{vShr,Exp}$	[0.1, 2.0]	4	0.1	[0.1,0.5]	3	0.1	0.4
$Mod_{Meander}$	1, 2, 3	3	3			3	1
$C_{Meander}$	[1.3, 2.2]	10	2.0			1.9	2.0
f_c	[0.00001, 0.005]	18	0.0003	[0.0001, 0.01]	19	0.0007	0.003

For the "Offset" grid search, the optimal values changed significantly from the first guess and ended up being higher in magnitude to better capture the wake deflection simulated by SOWFA. The optimal values for the "Eddy Viscosity and Near Wake" group turned out similar to the first guess, with a small reduction in magnitude. A valuable result from this calibration exercise is the disappearance of the ambient filter function from the eddy viscosity model, as can be seen by comparing its first guess and optimized form in Fig. 6a. This indicates that the ambient turbulence (as modeled) has the exact same contribution to the eddy viscosity at all downstream locations. The shear filter function changed substantially (Fig. 6b), ending up with higher $DMin$, $FMin$, and $DMax$ values. Conversely, the Exp value for the shear function was substantially reduced leading to a sharper transition between the near and the far wake at $x = DMin$.

The meandering grid search also yielded valuable results with $Mod_{Meander}$ option 3 and $C_{Meander} \sim 2.0$, yielding consistently the lowest error norms in both rounds. Option 3 defines a spatial averaging method for the disturbed wind field that weights each point in the domain using a windowed jinc function. The optimized constant of $C_{Meander} = 1.9$ results in a cutoff wave number of $\kappa_{cutoff} \sim (1/239)$ m^{-1} for the jinc function. High values of $C_{Meander}$ act to limit the magnitude of meandering by reducing this κ_{cutoff} value which distinguishes between energy roll off (at $\kappa < \kappa_{cutoff}$) and pockets of energy ($\kappa > \kappa_{cutoff}$). A

This report is available at no cost from the National Renewable Energy Laboratory at www.nrel.gov/publications.

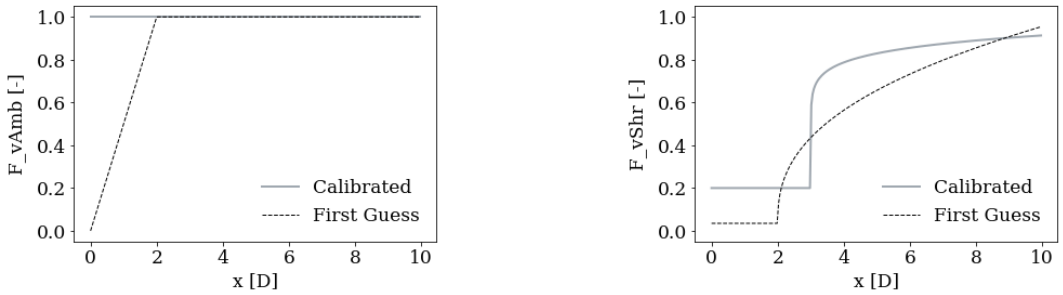

(a) Ambient Filter Function

(b) Shear Filter Function

Figure 6: Eddy viscosity filter functions for ambient (a) and wake shear layer (b) turbulence.

closer look at the error norms for the "Meandering" group at Round 2 (Fig. 7) revealed that the $C_{Meander}$ values should be chosen appropriately depending on the $Mod_{Meander}$ option selected, and that the error norm distribution as a function of $C_{Meander}$ is consistent across stratification and shear conditions. For option 1 (spatial average of disturbed wind with uniform weighting), the lowest error norms are seen close to $C_{Meander} = 1.6$ and for option 2 (jinc function weighting of each point, windowed by truncating it at its first zero crossing), close to $C_{Meander} = 1.7$.

Finally, the results of the "Transient" grid search reveal that high values of f_c (i.e., $f_c > 0.003$ Hz) result in meandering magnitudes that can be exceedingly large in the axial, lateral or vertical directions. These large wake motions can halt the execution of FAST.Farm if wake planes (on which calculations are performed) move too far below the ground in the vertical direction, or too close to an adjacent plane in the axial direction. In Round 1, a large sensitivity of error norms to f_c values was seen. In Round 2, this sensitivity is reduced likely to the better agreement found between FAST.Farm and SOWFA in yawed conditions after the calibration of the "Offset" group. After limiting the cutoff frequency to values below 0.003 Hz in Round 2 of the "Transient" grid search, $f_c = 0.0007$ Hz is found to be the optimal, calibrated value.

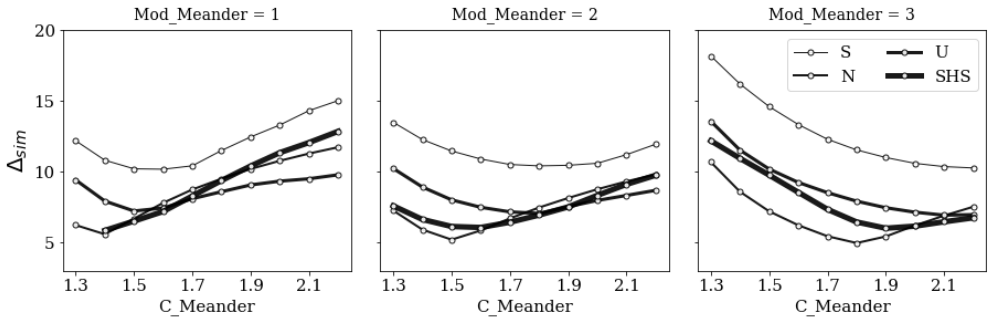

Figure 7: Error norm Δ_{sim} for each of the FAST.Farm simulations performed for the Round 2 grid search of the "Meandering" parameter group.

C. FAST.Farm Simulations with Optimized Parameter Values

1. Wake Meandering

Wake meandering for SOWFA and FAST.Farm using the optimized parameter values are given in Fig. 8. For lateral meandering, the agreement is substantially better than what was seen with the default parameter values both in terms of mean magnitude of meandering and of the spread of the distribution. The improvement is especially pronounced for the four yaw offset cases where $\Delta\mu_{wake}$ was reduced by $45 - 77\%$. For vertical meandering, improvement was also seen for all cases except `S`, which saw a reduction in $\Delta\sigma_{wake}$ but an increase in $\Delta\mu_{wake}$. In `S`, FAST.Farm continues to miss the fluctuations in meandering, and to overestimate

This report is available at no cost from the National Renewable Energy Laboratory at www.nrel.gov/publications.

the mean vertical displacement of the wake center relative to the hub. The minimal vertical deflection in SOWFA for the stable case is likely driven by a wake-induced boundary layer not captured by FAST.Farm.

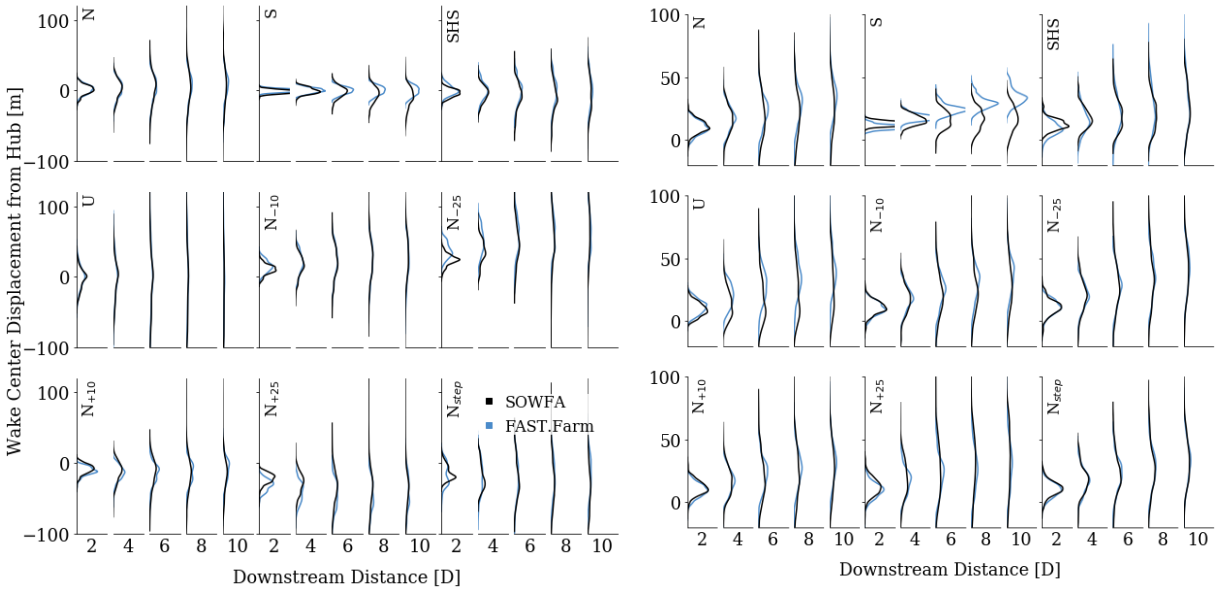

(a) Lateral Meandering

(b) Vertical Meandering

Figure 8: Axial evolution (primary horizontal axis, [D]) of fitted histograms (secondary horizontal axis) of wake center displacement (vertical axis,[m]) relative to WT hub in the lateral (a) and vertical (b) directions for the nine wake-simulation scenarios defined in Table 1 for SOWFA (black) and FAST.Farm (blue). Values are for FAST.Farm simulations run with the calibrated parameters. To enable direct comparisons, secondary horizontal axis spans 0.0 to 0.1 m^{-1} in (a) and (b). Vertical axes are uniform within (a) and within (b).

2. Wake Deficit

Radial profiles of mean wake deficit for FAST.Farm using the optimized parameter values are given in Fig. 9. There is a clear overall improvement in the simulation of axial deficits, especially in the near wake ($2-6$ D), and for the yaw offset scenarios. The improvement is less pronounced further downstream where FAST.Farm still over-estimates the axial deficit for the simulations with large yaw. The improvement in FAST.Farm predictions of radial velocity deficits is also clear, and seen for all simulations scenarios (yawed and not yawed) especially closer to the rotor where the first guess parameter values led to an over-prediction of the deficit recovery at distances $r > 0.5$ D from the wake center. This improvement can be quantified by the change in $\Delta\overline{\delta V}_r$ from the start to the end of the calibration. It reveals a reduction of at least 48% for all simulations except `U`, for which $\Delta\overline{\delta V}_r$ remained unchanged.

IV. Summary

The objective of the work presented herein was to calibrate FAST.Farm wake dynamics parameters relative to high-fidelity LES wake simulations. The calibration considered a variety of atmospheric conditions and turbine yaw settings (a range of conditions relevant for nominal and yawed wind farm operation), and consisted of performing a large number of FAST.Farm simulations in which groups of parameters were optimized sequentially using a grid search approach that was conducted twice. The grid search consisted of running a large number of simulations in which each parameter in the group was varied at a time, and then in determining which parameter configuration yielded the lowest error norm based on pre defined wake-characterization metrics. The methodology employed diagnoses these wake metrics from LES to match as closely as possible those computed within FAST.Farm.

Each error norm considered was weighted equally in the calibration procedure. As a result, whichever

This report is available at no cost from the National Renewable Energy Laboratory at www.nrel.gov/publications.

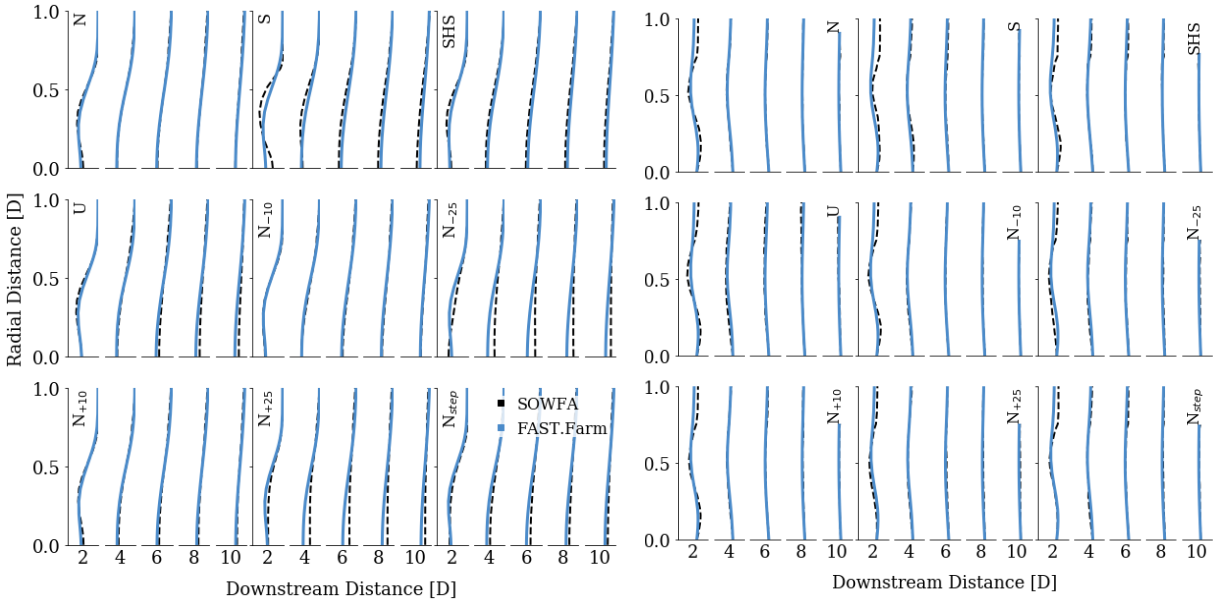

(a) Axial Velocity Deficit

(b) Radial Velocity Deficit

Figure 9: Axial evolution (primary horizontal axis, [D]) of radial distribution (vertical axis, [D]) of temporally averaged velocity deficit (secondary horizontal axis) in the axial (a) and radial (b) directions for the nine wake-simulation scenarios defined in Table 1 for SOWFA (black) and FAST.Farm (blue). Values are for FAST.Farm simulations run with the calibrated parameters. Secondary horizontal axis spans -5.5 to 0.1 m s^{-1} in (a) and -0.25 to 0.15 m s^{-1} in (b).

metric started out with the largest errors is the one that benefited the most from changes in the first-guess values for the parameters. Results indicated that this metric was the radial velocity deficit, which saw a consistent reduction in error norm across the simulation scenarios and yaw angles considered.

Because the simulations conducted did not include the Coriolis effect, it was necessary to force two offset parameters to zero in order to calibrate the other two. Namely, the parameters that prescribe a consistent offset in the wake position were set to zero, and those that are dependent on yaw angle were allowed to vary. These calibrated offset parameters turned out to be larger in magnitude than the first guess, and yielded much better agreement in meandering statistics between FAST.Farm and SOWFA. The parameters in the "Eddy Viscosity and Near Wake" group remained similar to the first-guess values. The filter function for the contribution of ambient turbulence to the eddy viscosity closure was removed from the model according to the optimized values. This was a significant result and reduced the number of parameters from 18 to 14. The largest change in the wake shear turbulence filter function was in the exponent, substantially modifying the function shape.

The calibrated parameters seemed to be robust for the wide range of simulation scenarios considered, as was verified in the second round of the sequential grid search in which little variation was seen in the evolution of error norms as different groups are calibrated. The calibrated parameters resulting from this work will be used for the subsequent FAST.Farm validation, which will consider other atmospheric conditions, multiple wakes, and large wind farms.

Acknowledgements

The authors acknowledge the support of Sang Lee, Matt J. Churchfield, and Eliot Quon of NREL in assisting with the numerical simulations performed for this study. Peer review was conducted by Senu Sirnivas of NREL and Jonas Kazda of DTU. Aditya Ghate acknowledges the support received from the Tomkat Center for Sustainable Energy at Stanford University. This work was supported by the U.S. Department of Energy under Contract number DE-AC36-08GO28308 with Alliance for Sustainable Energy, LLC, the Manager and

This report is available at no cost from the National Renewable Energy Laboratory at www.nrel.gov/publications.

Operator of the National Renewable Energy Laboratory. Funding was additionally provided by an NREL Laboratory Directed Research and Development (LDRD) grant titled, "Multi-Physics Engineering Tool for Wind-Plant Design and Analysis." The U.S. Government retains and the publisher, by accepting the article for publication, acknowledges that the U.S. Government retains a nonexclusive, paid-up, irrevocable, worldwide license to publish or reproduce the published form of this work, or allow others to do so, for U.S. Government purposes.

This report is available at no cost from the National Renewable Energy Laboratory at www.nrel.gov/publications.

References

[1]Gaumond, M., Réthoré, P.-E., Ott, S., Peña, A., Bechmann, A., and Hansen, K. S., "Evaluation of the wind direction uncertainty and its impact on wake modeling at the Horns Rev offshore wind farm," *Wind Energy*, Vol. 17, No. 8, Aug. 2014, pp. 1169–1178.

[2]Gebraad, P. M. O., Teeuwisse, F. W., van Wingerden, J. W., Fleming, P. A., Ruben, S. D., Marden, J. R., and Pao, L. Y., "Wind plant power optimization through yaw control using a parametric model for wake effects—a CFD simulation study," *Wind Energ.*, Vol. 19, No. 1, Jan. 2016, pp. 95–114.

[3]Hao, Y. and Lackner, M. A., "Wind farm wake modeling using NWTC design codes," *Wind Engineering*, Vol. 41, No. 1, Feb. 2017, pp. 62–73.

[4]Hahn, S., Machefaux, E., Hristov, Y. V., Albano, M., and Threadgill, R., "Estimation of annual energy production using dynamic wake meandering in combination with ambient CFD solutions," *J. Phys.: Conf. Ser.*, Vol. 753, No. 3, 2016, pp. 032043.

[5]Vijayakumar, G., Brasseur, J., Lavely, A. W., Jayaraman, B., and Craven, B., "Interaction of atmospheric turbulence with blade boundary layer dynamics on a 5MW wind turbine using blade-boundary-layer-resolved CFD with hybrid URANS-LES," American Institute of Aeronautics and Astronautics, Jan. 2016.

[6]Churchfield, M. J., Lee, S., Michalakes, J., and Moriarty, P. J., "A numerical study of the effects of atmospheric and wake turbulence on wind turbine dynamics," *Journal of Turbulence*, Vol. 13, Jan. 2012, pp. N14.

[7]Jonkman, J. M., Annoni, J., Hayman, G., Jonkman, B., and Purkayastha, A., "Development of FAST.Farm: a new multi-physics engineering tool for wind-farm design and analysis," *35th Wind Energy Symposium*, American Institute of Aeronautics and Astronautics, 2017, DOI: 10.2514/6.2017-0454.

[8]Clifton, A., Smith, A., and Fields, M., "Wind plant preconstruction energy estimates: current practice and opportunities," Technical Report NREL/TP–5000-64735, National Renewable Energy Laboratory, Golden, CO, 2016.

[9]Doubrawa, P., Barthelmie, R. J., Wang, H., and Churchfield, M. J., "Contributions of the stochastic shape wake model to predictions of aerodynamic loads and power under single wake conditions," *J. Phys.: Conf. Ser.*, Vol. 753, No. 8, 2016, pp. 082006.

[10]Ghate, A. S. and Lele, S. K., "A modeling framework for wind farm analysis: wind turbine wake interactions," American Institute of Aeronautics and Astronautics, Jan. 2015.

[11]Annoni, J., Gebraad, P. M., Scholbrock, A. K., Fleming, P. A., and Wingerden, J.-W. v., "Analysis of axial-induction-based wind plant control using an engineering and a high-order wind plant model," *Wind Energy*, 2015.

[12]Jonkman, J. M. and Buhl Jr., M. L., "FAST user's guide," Technical Report NREL/EL-500-38230, National Renewable Energy Laboratory, Golden, Colorado, Aug. 2005.

[13]Larsen, G. C., Madsen Aagaard, H., Bingöl, F., Mann, J., Ott, S., Sørensen, J. N., Okulov, V., Troldborg, N., Nielsen, N. M., and Thomsen, K., "Dynamic wake meandering modeling," Tech. rep., Risø National Laboratory, 2007.

[14]Ainslie, J. F., "Calculating the flowfield in the wake of wind turbines," *Journal of Wind Engineering and Industrial Aerodynamics*, Vol. 27, No. 1–3, Jan. 1988, pp. 213–224.

[15]Churchfield, M., Lee, S., Moriarty, P., Martinez, L., Leonardi, S., Vijayakumar, G., and Brasseur, J., "A large-eddy simulation of wind-plant aerodynamics," *50th AIAA Aerospace Sciences Meeting including the New Horizons Forum and Aerospace Exposition*, 2012, p. 537.

[16]Haupt, S., Kotamarthi, R., Feng, Y., Mirocha, J., Koo, E., Linn, R., Kosovic, B., Brown, B., Anderson, A., Churchfield, M., Draxl, C., Quon, E., Shaw, W., Berg, L., Raiand, R., and Ennis, B., "Second year report of the Atmosphere to Electrons Mesoscale to Microscale Coupling project: nonstationary modeling techniques and assessment," Tech. Rep. PNNL-26267, Pacific Northwest National Laboratory, Richland, Washington, 2017.

[17]Jonkman, B. J., "TurbSim user's guide: Version 1.50," 2009.

[18]Sørensen, J. N. and Shen, W. Z., "Numerical modeling of wind turbine wakes," *J. Fluids Eng*, Vol. 124, No. 2, May 2002, pp. 393–399.

This report is available at no cost from the National Renewable Energy Laboratory at www.nrel.gov/publications.